BBC RD 1973/18

Engineering Research Report

The work covered by this report was undertaken by the BBC Research Department for the BBC and the IBA

# The automatic plotting of aerial radiation patterns

G.H. Millard, B.Sc., M.Inst.P.
N.F. Spring, B.Sc., A.R.C.S., M.Inst. P.

Research Department, Engineering Division
THE BRITISH BROADCASTING CORPORATION August 1973

**BBC RD 1973/18**
UDC 621.396.677
621.3.095.4

# THE AUTOMATIC PLOTTING OF AERIAL RADIATION PATTERNS

**G.H. Millard, B.Sc., M.Inst.P.**
**N.F. Spring, B.Sc., A.R.C.S., M.Inst.P.**

## Summary

*The presentation of aerial radiation patterns in the form of contour plots is described and a brief account is given of the plotting algorithm.*

Issued under the authority of

P. Rainger

Head of Research Department

**Research Department, Engineering Division,**
**BRITISH BROADCASTING CORPORATION**
August 1973
(RA-114)

# THE AUTOMATIC PLOTTING OF AERIAL RADIATION PATTERNS

| Section | Title | Page |
|---|---|---|
| | Summary | Title Page |
| 1. | Introduction | 1 |
| 2. | Radiation patterns of UHF aerials | 1 |
| 3. | The polar-contour plot | 1 |
| 4. | The plotting algorithm | 2 |
| 5. | Calculation of the radiation pattern matrix | 7 |
| 6. | Implementation of plotting algorithm | 8 |
| 7. | Conclusions | 8 |
| 8. | References | 9 |

**BBC RD 1973/18**
UDC 621.396.677
621.3.095.4

# THE AUTOMATIC PLOTTING OF AERIAL RADIATION PATTERNS

**G.H. Millard, B.Sc., M.Inst.P.**
**N.F. Spring, B.Sc., A.R.C.S., M.Inst.P.**

## 1. Introduction

It has been common practice in the past to represent an aerial radiation pattern in terms of separate horizontal and vertical patterns, it being tacitly assumed that the field in any other direction would be given by the product of the two. A common form of presentation is the polar plot on which field strength at a constant distance is represented linearly on the radius co-ordinate. An example is shown in Fig. 1 of a horizontal pattern of this type. The polar/voltage diagram is not very satisfactory when it is desired to show the performance of a very directional aerial. In Fig. 1 it will be seen that the field in the minima cannot be read with any great accuracy and to overcome this difficulty the polar plot is sometimes shown with a logarithmic radial scale. A better arrangement is to use cartesian rather than polar co-ordinates for the logarithmic plot. This has the advantage that the angular scale can be chosen to suit the aerial; in particular an expanded scale can be used for an aerial with a very narrow beam. Fig. 2 shows the radiation pattern of Fig. 1 in this form. This diagram is used in connection with the automatic measurement of aerial radiation patterns.

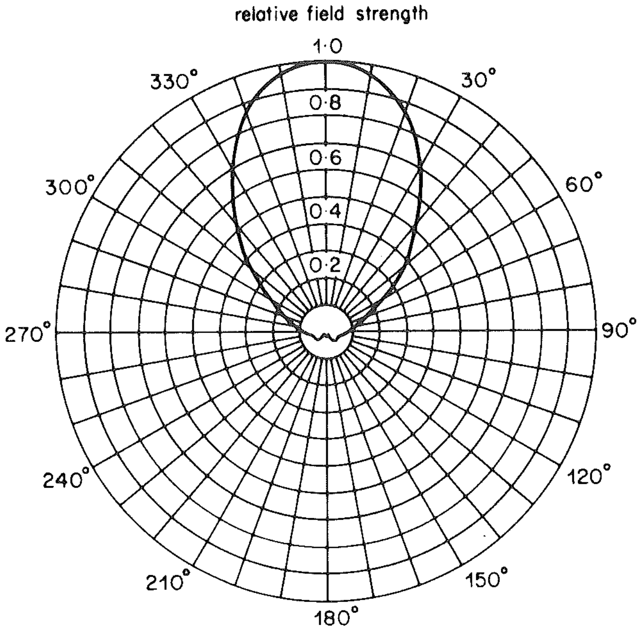

*Fig. 1 - Polar-voltage diagram (u.h.f. panel aerial)*

The use of two sections at right-angles (i.e. the radiation patterns in the horizontal and vertical planes) to represent a three-dimensional radiation pattern is acceptable only in special cases. With a complex array having a multi-lobed radiation pattern a different presentation must be used. A diagram which is sometimes used to illustrate the performance of large high-frequency arrays is the power distribution diagram (sometimes called an 'onion diagram') shown in Fig. 3. The characteristic shape arises because the length of the lines of latitude are proportional to the sine of the latitude; as a result, areas on this chart are equal to the corresponding areas on the surface of the corresponding sphere. The radiation pattern of the aerial is shown in the form of contours of equal field strength or power flow; if the latter are plotted the diagram may be used to deduce the gain of the array by graphical integration.[1]

## 2. Radiation patterns of UHF aerials

Certain difficulties arise in the presentation of radiation patterns of u.h.f. aerials. First, the aerials are often several wavelengths long so that there is considerable detail in the patterns. Second, the maximum field in any vertical plane is normally arranged to fall at some arbitrary angle below the horizontal, known as the beam-tilt angle. Where a 'horizontal' radiation pattern is required it is usually measured or calculated at the beam-tilt angle. However, at some stations the beam tilt angle may vary with azimuth so that an adequate representation of the three-dimensional radiation pattern would need several 'horizontal' radiation patterns corresponding to several angles in the vertical plane. Diagrams comprising several such patterns superposed have been produced for particular aerials but they are not easy to interpret. It was this consideration together with the need to be more specific about the detailed structure of radiation patterns which led to the devising of a new form of representation.

## 3. The polar-contour plot

A number of basic requirements were laid down for the new form of presentation. First, all the relevant information relating to the radiation pattern had to be condensed onto one diagram. Second, the diagram needed to have a pictorial quality so that the reader could readily visualise what was represented. Third, the diagram needed to yield

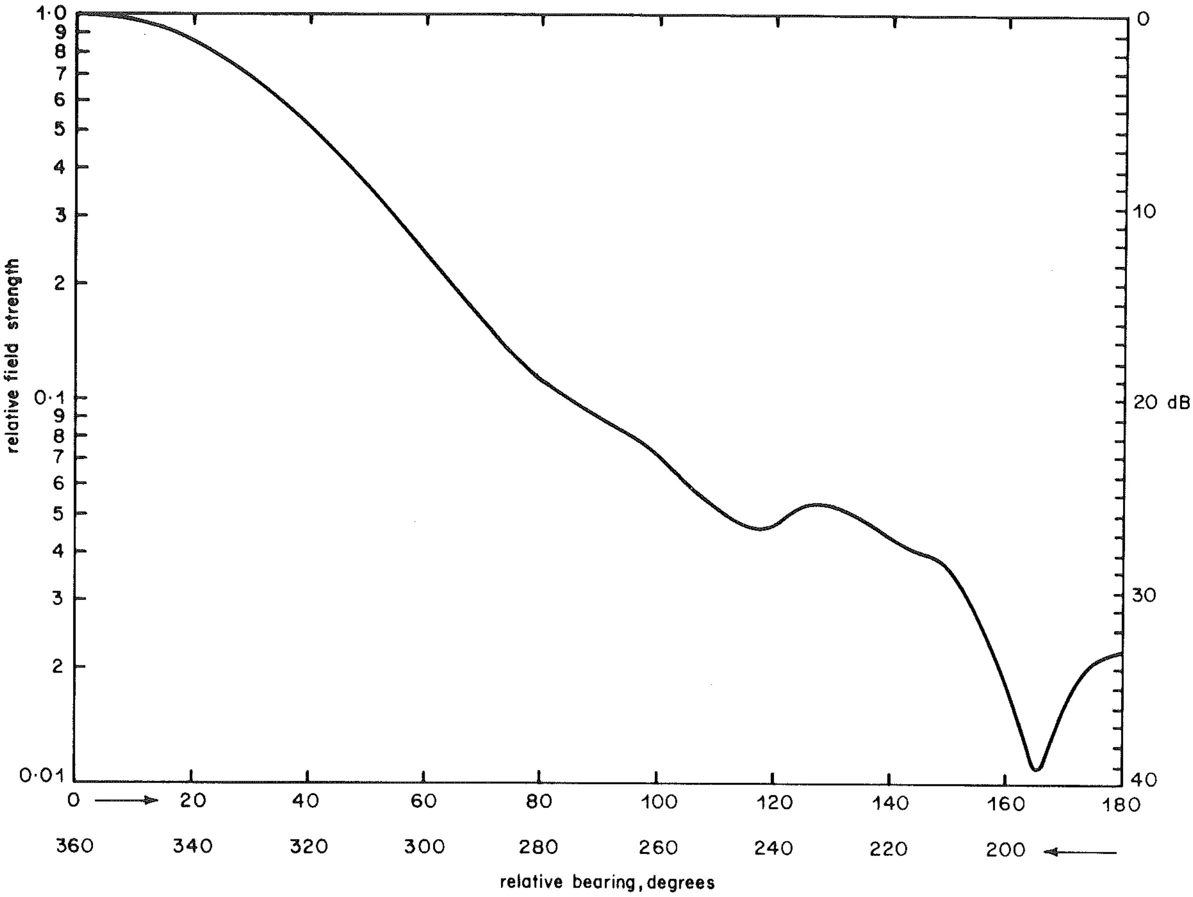

*Fig. 2 - Cartesian-logarithmic diagram (u.h.f. panel aerial)*

decibel values of field strength readily so that it would be easy to use in predicting field strength. Finally, it was desired to be able to produce the diagram directly from a computer. This latter requirement meant that diagrams could be considered which would have been unduly time-consuming to produce by hand.

The form of diagram* meeting these requirements is shown in Fig. 4. The polar angle corresponds to the angle of azimuth with the cardinal points of the compass marked. The radial distance corresponds to the angle below the horizontal, the outermost circle corresponding to the horizontal. The range of vertical angles shown (0° to 20°) is chosen to include those angles of greatest interest at the majority of stations.

Fig. 5 shows the representation of a typical aerial. The contours are of equal field strength and are shown in decibels below the maximum. The whole diagram may be considered as representative of the way the aerial distributes energy over the service area.

A more complicated example is given in Fig. 6; the diagram shows clearly areas of low field strength which might easily have been overlooked with other forms of presentation.

## 4. The plotting algorithm

It was required to produce a plot of contours of constant effective radiated power from a matrix containing samples of the radiation pattern for the appropriate range of azimuthal and zenithal angles. Such a programme could be adapted to plot contours of any function of the form $Z = f(\theta, \phi)$ where $Z$ is the 'height' of a contour.

The task of devising a contour-plotting algorithm is full of pitfalls for the unwary. The basic problem is to ensure that no contours of a given height are overlooked in the area under construction, that no contours are drawn more than once, and that those conditions are fulfilled without consuming unacceptable amounts of computer storage and run-time.

Consider a rectangular area ABCD (Fig. 7) divided up into a rectangular grid. It is assumed that the values of $Z$ are known at every intersection-point on the grid and that it is required to plot all the contours of a 'height' $Z = Z_0$ over the area ABCD. The procedure is as follows:

i) Mark every intersection where $Z \geqslant Z_0$ with the label 'high'. Mark all others 'low'.

ii) Scan every horizontal side of the elemental rectangles (such as ab and cd) except those on the boundaries AB and CD. Whenever a 'high' intersection has a

---

* First proposed by R.I. Black.

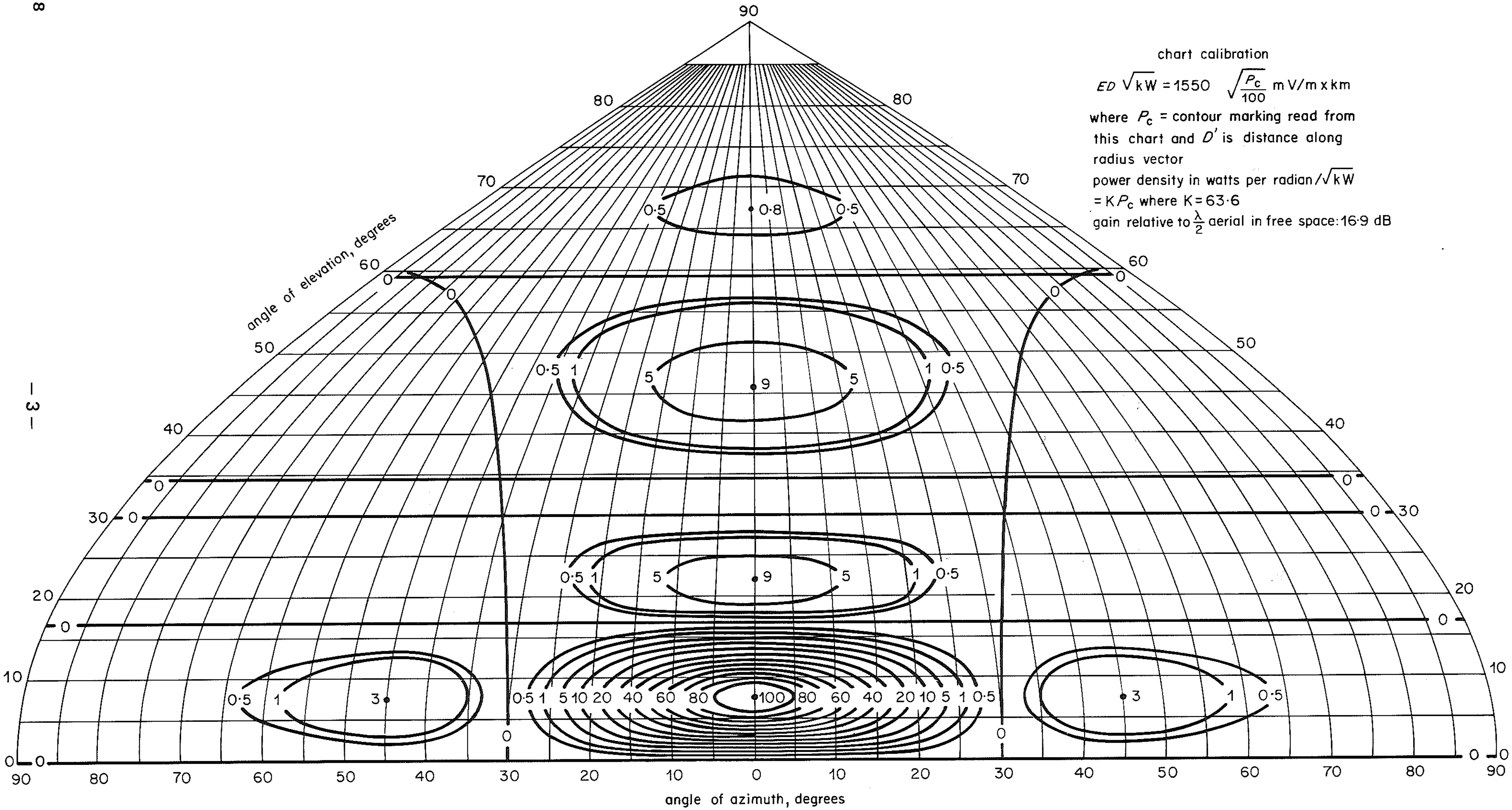

chart calibration

$ED\sqrt{\mathrm{kW}} = 1550 \quad \sqrt{\frac{P_c}{100}}$ mV/m x km

where $P_c$ = contour marking read from this chart and $D'$ is distance along radius vector

power density in watts per radian/$\sqrt{\mathrm{kW}}$ = $KP_c$ where K = 63·6

gain relative to $\frac{\lambda}{2}$ aerial in free space: 16·9 dB

*Fig. 3 - Power distribution diagram: antenna array H4/4/1*

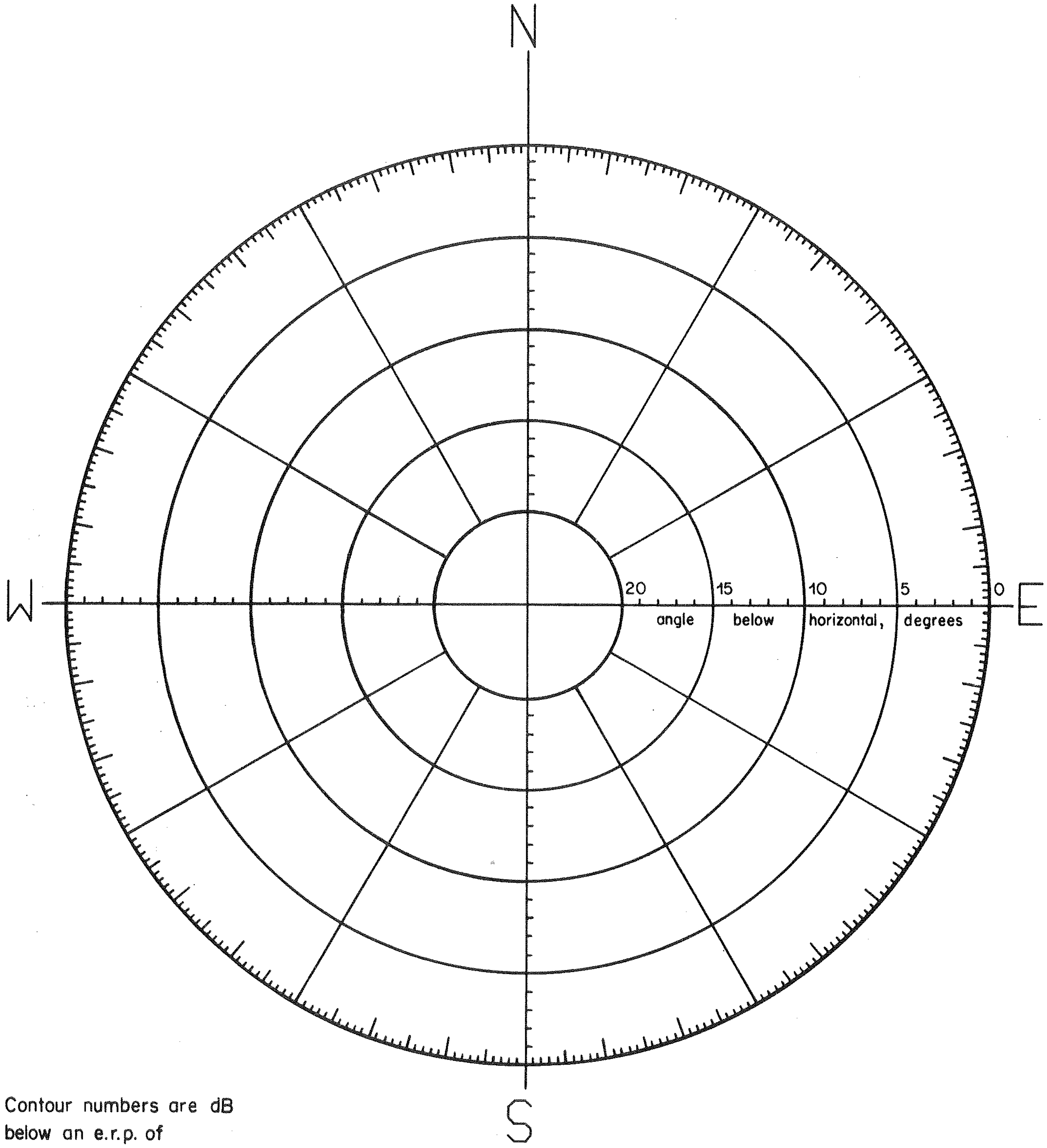

Contour numbers are dB
below an e.r.p. of

*Fig. 4 - Graticule for polar/contour plot*

08 NOV 72

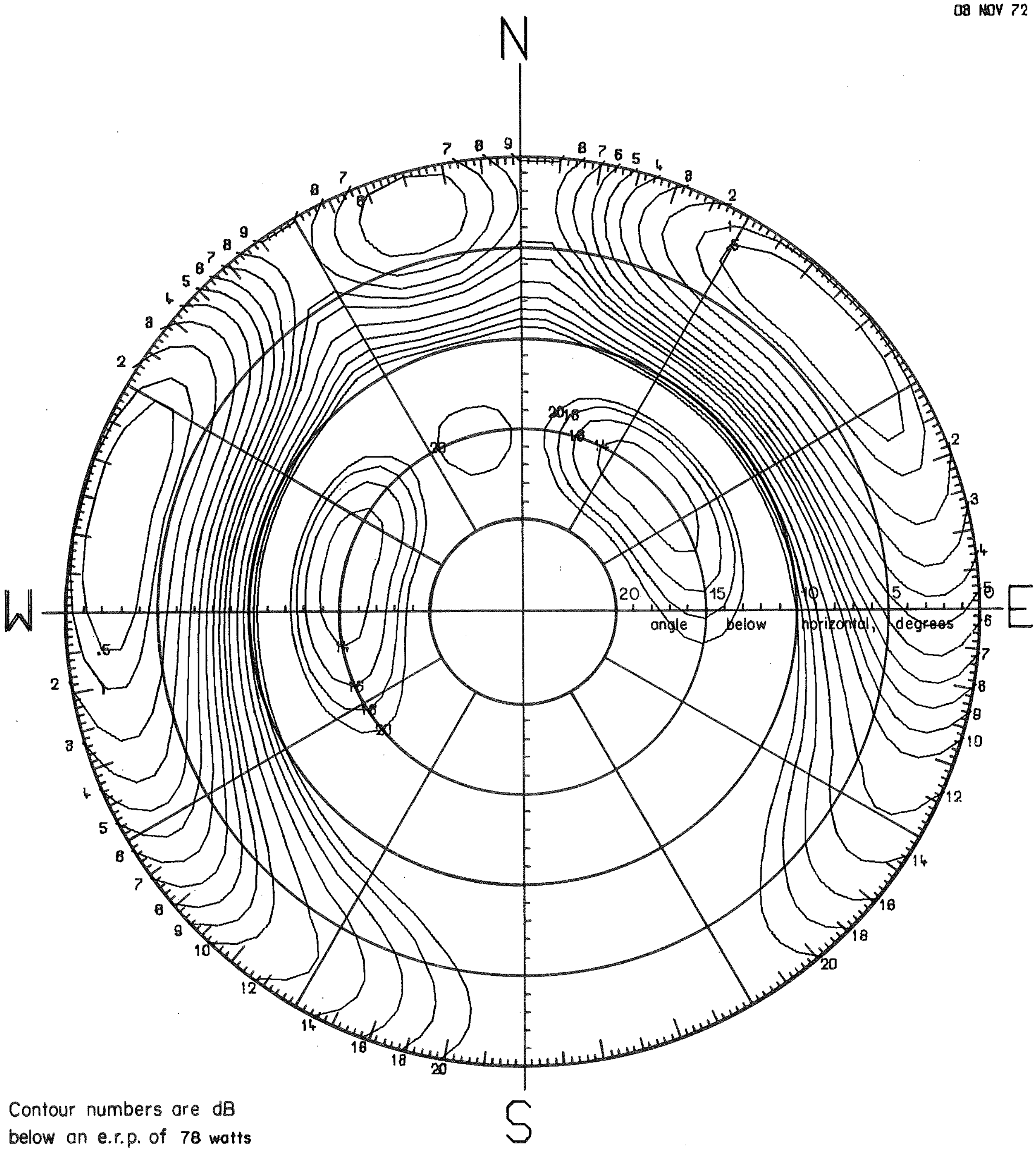

Contour numbers are dB
below an e.r.p. of 78 watts

110.03 WESTWOOD 4 TIERS PANELS CHANNEL 40 AE 1338

*Fig. 5 - Polar/contour plot: 4 tiers each of two panels set at 120°, 2·5° beam tilt*

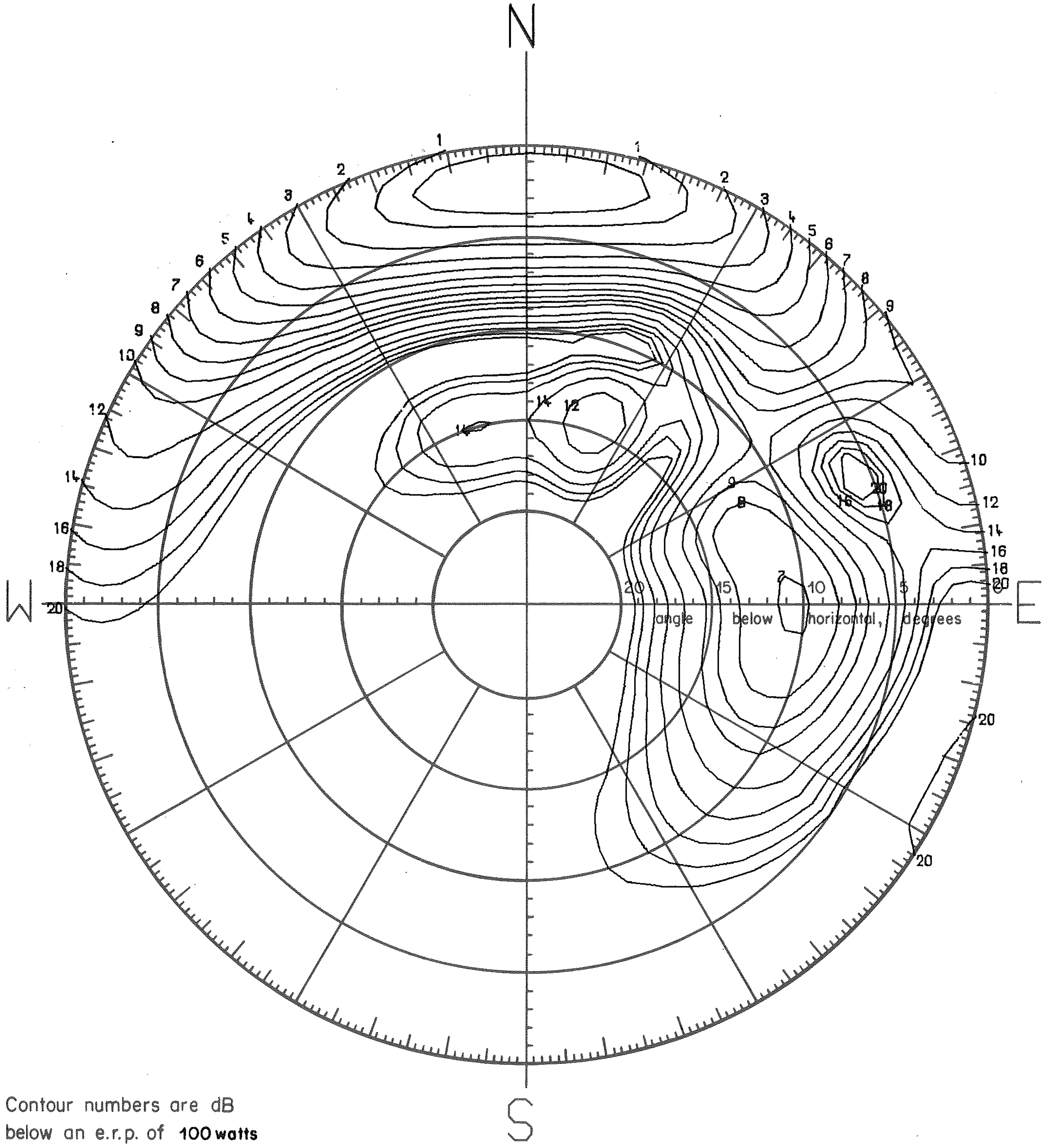

Contour numbers are dB below an e.r.p. of **100 watts**

103.31 BBC UHF PANEL AERIAL CH.41

*Fig. 6 - Polar/contour plot: 4 tiers each of two panels on 0° and 90° ETN. Panels on 0° carry unit power and have beam tilt of 2°. Panels on 90° carry quarter power and have beam tilt of 12°*

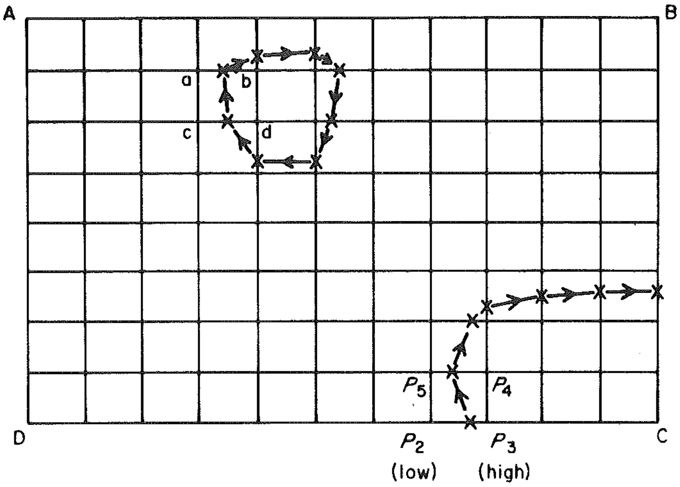

*Fig. 7 - Method of drawing contours*

'low' intersection immediately to the left of it, mark the 'high' intersection as 'uncrossed'.

iii) Contours starting and finishing on the boundary ABCD are now drawn, as follows. Examine the intersections of the grid-lines with the boundary ABCD until there is found a pair for which, from the viewpoint of an observer outside the boundary, the right-hand intersection is marked 'high' and the left-hand intersection is marked 'low'. $P_2$ and $P_3$ in Fig. 1 are such a pair. The start of the contour is obtained by inverse interpolation of $Z_0$ between the values of $Z$ at $P_2$ and $P_3$. If $P_4$ is 'low' the contour is assumed to exit $P_2$ $P_3$ $P_4$ $P_5$ via the side $P_3$ $P_4$. If not, then $P_5$ is examined to see whether the exit is via $P_4$ $P_5$ or $P_2$ $P_5$.

On whatever side the exit occurs, a new $P_2$ $P_3$ $P_4$ $P_5$ rectangle is set up and the process repeated until the boundary ABCD is reached.

In tracing out a contour, whenever a horizontal edge is traversed upwards, then the label 'uncrossed' at the right-hand end is changed to 'crossed'. The remainder of the boundary ABCD is scanned systematically for starts of other contours.

iv) Having drawn all the contours which terminate on the boundary ABCD ('open' contours), it is now necessary to find those which do not ('closed' contours). This is done by scanning the internal horizontal edges (such as ab or cd) until one is found for which the right-hand end is marked 'uncrossed'. A test rectangle $P_2P_3P_4P_5$ is then erected on top of this edge and the contour followed in the same way as for open contours. However, the test for terminating a closed contour is that a horizontal edge is encountered such that its right-hand end is marked 'crossed'. The rest of the internal horizontal edges are scanned and closed contours plotted until there are no 'uncrossed' edges left.

v) The whole of the above procedure is repeated for each different contour height.

Note that the contours are shown as being made up of straight lines joining the intersections of the contours with the grid. This has the advantages of simplicity and the assurance that contours will never intersect each other (although they may touch each other).[2] Judicious choice of cell-size in the grid makes the straight line method satisfactory for most contours. It is thought that the expense of curve-drawing procedures would not be justified.

## 5. Calculation of the radiation pattern matrix

The radiation pattern is evaluated from the formula

$$E_j = \sum_i A_i R_{ij} e^j \left\{ Q_i + P_{ij} \frac{2\pi}{\lambda} (l_j x_i + m_j y_i + n_j z_i) \right\}$$

| | |
|---|---|
| where $\lvert E_j \rvert$ | is the field intensity in direction $(\theta_j', \phi_j')$ |
| $(\theta_j', \phi_j')$ | are a set of directions in spherical-polar co-ordinates |
| $(l_j, m_j, n_j)$ | are the direction cosines of $(\theta_j', \phi_j')$ |
| $A_i e^{jQ_i}$ | is the current in the ith source |
| $R_{ij} e^{jP_{ij}}$ | is the radiated field intensity of source no. i in direction $(\theta_j', \phi_j')$ |
| $(x_i, y_i, z_i)$ | are the cartesian co-ordinates of the position of source no. i. |

It is assumed that for each source the co-ordinate $(x_i, y_i, z_i)$, the current $A_i e^{jQ_i}$, the direction of fire $(\theta_i, \phi_i)$ are given and the radiation pattern $Re^{jP}$ is given (relative to the 'natural axes' of the source) as a function of $(\theta, \phi)$. If the source is 'turned' through an angle $\phi_i$ and 'tilted' through an angle $\theta_i$ (see Fig. 8), then to determine $Re^{jP}$ in direction $(\theta_j' \ \phi_j')$ it is necessary to evaluate the co-ordinate $(\theta_{ij}'' \ \phi_{ij}'')$ of the direction $(\theta_j', \phi_j')$ relative to $(\theta_i, \phi_i)$. The appropriate formulae were determined using the formulae of spherical trigonometry and are given below:

$$\cos\theta_{ij}'' \cos\phi_{ij}'' = \sin\theta_j' \sin\theta_i + \cos\theta_j' \cos\theta_i \sin(\phi_j' - \phi_i)$$

$$\cos\theta_{ij}'' \sin\phi_{ij}'' = \cos\theta_j' \sin(\phi_j' - \phi_i)$$

$$\sin\theta_{ij}'' = \sin\theta_j' \cos\theta_i - \cos\theta_j' \sin\theta_i \cos(\phi_j' - \phi_i).$$

For the purposes of this programme the axes and co-ordinates are slightly non-standard. OX, OY, OZ are mutually orthogonal cartesian axes with OZ pointing vertically upwards. The spherical polar co-ordinates $(\theta \ \phi)$ are such that $\phi$ is measured from OX towards OY and lies between 0° and 360°, and $\theta$ is measured from the horizontal towards OZ and lies between $-90°$ and $+90°$; +ve angles are above the horizontal and −ve angles below.

It should be noted that individual sources could have a further angular degree of freedom apart from 'turn', $\phi$, and 'tilt', $\theta$. This might be described as 'twist' about the direction of fire. This parameter has been excluded from the present programme because it would be necessary to evaluate both planes of polarisation.

The most commonly used source at low power relay stations is the printed panel aerial.[3] Radiation pattern data

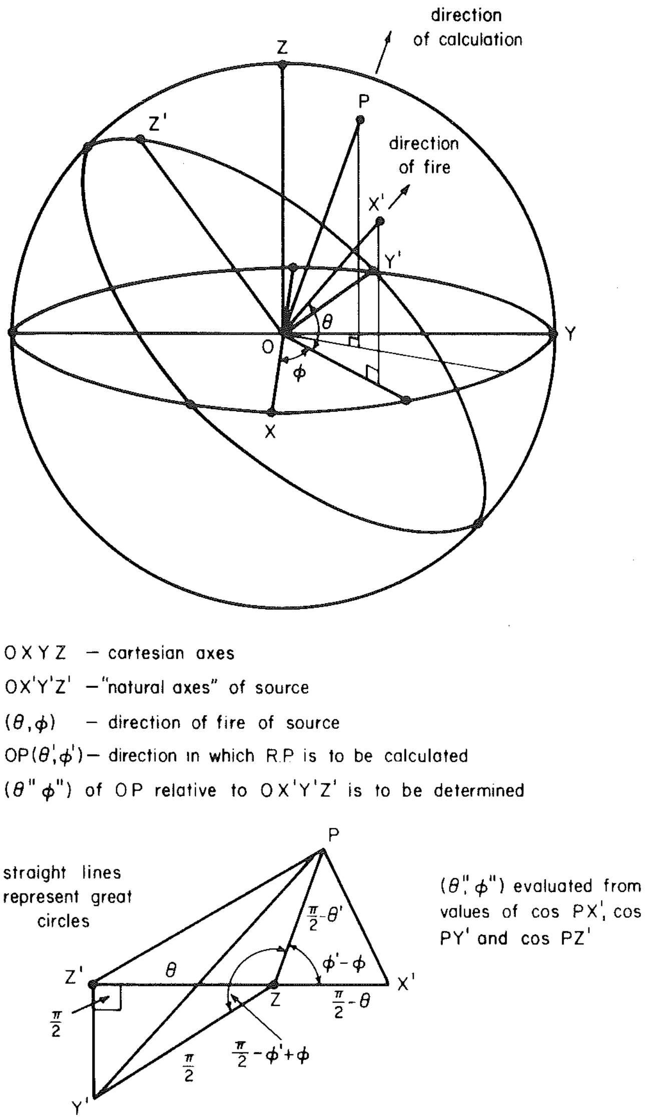
direction
of calculation
Z
P
Z'
direction
of fire
X'
Y'
θ
O
φ
Y
X
OXYZ – cartesian axes
OX'Y'Z' – "natural axes" of source
(θ,φ) – direction of fire of source
OP(θ',φ') – direction in which R.P. is to be calculated
(θ'' φ'') of OP relative to OX'Y'Z' is to be determined
P
straight lines represent great circles
(θ'' φ'') evaluated from values of cos PX', cos PY' and cos PZ'
Z'
θ
π/2-θ'
φ'-φ
X'
Z
π/2-θ
π/2
π/2
π/2-φ'+φ
Y'

*Fig. 8 - Calculation of relative θ, φ*

for this aerial at a number of frequencies are stored in the computer along with the programme. This results in a great reduction of the number of data cards to be prepared for each calculation on arrays of this aerial.

## 6. Implementation of plotting algorithm

The algorithm described in Section 4 has been followed broadly in the contour-plotting subroutine but there are some minor differences. In particular, the area over which contours are drawn is circular, not rectangular. For the contouring algorithm, the polar pattern is cut along the North radius and opened out into a rectangle as shown in Fig. 9.

Another difference is that, when the grid is being scanned for contour starts, each part of the grid is examined for each contour height in turn before moving to the next part of the grid. As a consequence, marks 'high', 'low', 'crossed' and 'uncrossed' must be stored for each contour height.

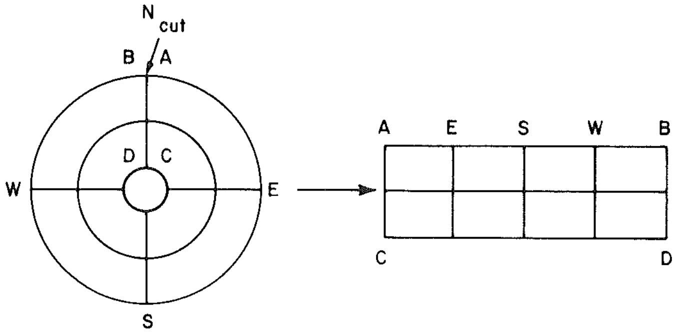

*Fig. 9 - Conversion of polar to rectangular grid*

Provision is made for plotting two sizes of the diagram. The smaller is contained within A4 size paper and is intended for record purposes. The larger, which is almost twice the size, is intended for those cases where detailed work has to be done using the diagram. Either diagram, or both, may be plotted as required.

The programme is written in Fortran V.*

Figs. 5 and 6 show the most commonly used ranges of vertical and horizontal angles. Any other vertical range extending over not more than 20° may be provided and the azimuth angle may be restricted if so desired. The cell size of the grid must be chosen sufficiently fine in relation to the expected complexity of the radiation pattern to avoid overlooking significant detail. Intervals of 1° in the zenithal angle and 5° in the azimuthal angle were chosen for Figs. 5 and 6. In practice, a plot in which the straight segments of the contours are not unduly obtrusive is unlikely to omit significant detail.

The computer programme is arranged to draw the graticule in a different colour to the contours. If, however, it is desired to produce many copies of a diagram, it is more economical to produce a plot of the contours only and then to print this onto blank graticules. In order to facilitate this operation, the letters labelling the cardinal points of the compass are drawn by both the contour- and the axes-plotting routines and are then available as registration marks. Figs. 5 and 6 have been reproduced in this way.

## 7. Conclusions

A new form of aerial radiation pattern diagram has been devised to give more complete and accurate information of aerial performance. A computer programme has been written in Fortran V which calculates the aerial radiation pattern and plots it in the new form.

*The programme calculating the radiation pattern matrix and the first version of the plotting programme were written by R.E. Davies.

## 8. References

1. PAGE, H. 1963. An introduction of the theory of aerials. BBC Research Department Report No. E-085, Serial No. 1963/27.

2. HEAP, B.R. *and* PINK, Monica, G. 1969. Three contouring algorithms. DNAM Report 81, Division of Numerical and Applied Mathematics, National Physical Laboratory, December 1969.

3. MILLARD, G.H. 1970. U.H.F. relay stations: vertically polarized printed panel aerial. BBC Research Department Report No. 1970/17.

SMW/JUC

Printed by BBC Research Department, Kingswood Warren, Tadworth, Surrey